JOC The Journal of Organic Chemistry

Note

pubs.acs.org/joc

Synthesis and Characterization of RNA Containing a Rigid and Nonperturbing Cytidine-Derived Spin Label

Claudia Höbartner,*[,†] Giuseppe Sicoli,[‡] Falk Wachowius,[†] Dnyaneshwar B. Gophane,[§] and Snorri Th. Sigurdsson*[,§]

[†]Max Planck Research Group Nucleic Acid Chemistry and [‡]Research Group Electron Paramagnetic Resonance, Max Planck Institute for Biophysical Chemistry, Am Fassberg 11, 37077 Göttingen, Germany

[§]Science Institute, University of Iceland, Dunhaga 3, 107 Reykjavik, Iceland

Supporting Information

ABSTRACT: The nitroxide-containing nucleoside **Çm** is reported as the first rigid spin label for paramagnetic modification of RNA by solid-phase synthesis. The spin label is well accommodated in several RNA secondary structures as judged by its minor effect on the thermodynamic stability of hairpin and duplex RNA. Electron paramagnetic resonance (EPR) spectroscopic characterization of mono-, bi-, and trimolecular RNA structures shows that **Çm** will be applicable for advanced EPR studies to elucidate structural and dynamic aspects of folded RNA.

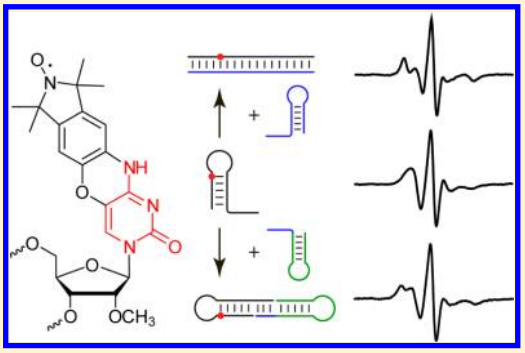

Nitroxide spin labels have found widespread applications as probes for examination of both structure and dynamics of biomolecules by EPR spectroscopy. In site-directed spin labeling (SDSL), nitroxide probes are inserted at specific positions in macromolecules, often through postsynthetic labeling of prefunctionalized sites.[1−4] For RNA, such functionalized modifications include 2′-amino-modified pyrimidine nucleotides,[5,6] the phosphorothioate backbone,[7,8] and 5-iodopyrimidine or 2-iodoadenine.[9,10] Alternatively, spin labels are postsynthetically incorporated into RNA via convertible nucleosides.[11] This strategy yields spin-labeled nucleoside N^4-TEMPO-cytidine ($\mathbf{C^T}$) which contains the nitroxide label attached at the exocyclic amino group of the nucleobase (Figure 1). Postsynthetic modification strategies are usually tied to the installation of flexible or semirigid tethers between the attachment site and the nitroxide. Despite the adaptability of flexible linkers and labels to structural constraints, rotational freedom of the spin label can complicate the analysis of EPR experiments.[12] Although the number of reports on structural investigations on RNA by EPR spectroscopy using established spin labels is increasing,[13−15] new EPR techniques and instrumentation[16] demand the development of new rigid spin labels for RNA.[17]

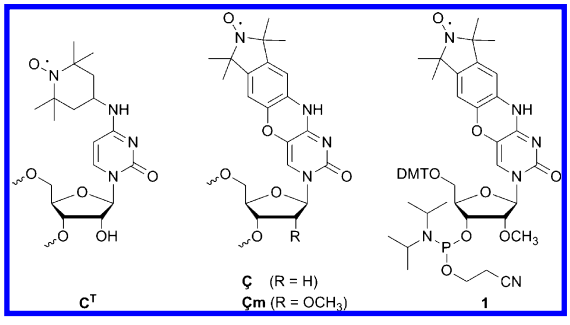

Figure 1. Nitroxide-containing cytidine derivatives and the phosphoramidite **1** for incorporation of **Çm** into RNA.

Here, we report the 2′-*O*-methylribonucleoside **Çm** as rigid spin label for paramagnetic labeling of RNA. Efficient incorporation of **Çm** into RNA by solid-phase synthesis via compound **1** provides the first example of RNA spin labeling using the phosphoramidite approach. The design of the spin label **Çm** was inspired by the 2′-deoxyribonucleoside **Ç** ("C-spin", Figure 1), a rigid spin label for DNA in which the nitroxide is fused to the nucleobase to form a phenoxazine derivative.[18−22]

Çm was prepared from 2′-*O*-methyluridine (**Um**) in eight steps (Scheme 1), starting with bromination of **Um** at position 5 to give 5-bromo-2′-*O*-methyluridine (**2**). Activation of **2** with PPh_3/CCl_4, followed by coupling with the tetramethyl isoindoline derivative **5** in the presence of DBU, which was used to make **Ç**,[19] gave low yields of **6**. Instead, the protected 5-bromouridine derivative **3** was chlorinated at position 4[23] to yield the dihalogenated nucleoside **4**. Upon reaction with the tetramethyl isoindoline derivative **5**, the first nucleophilic substitution occurred at the most reactive position of the pyrimidine heterocycle. Treatment of compound **6** with

Received: June 23, 2012
Published: August 12, 2012

Scheme 1. Synthesis of Çm Phosphoramidite 1

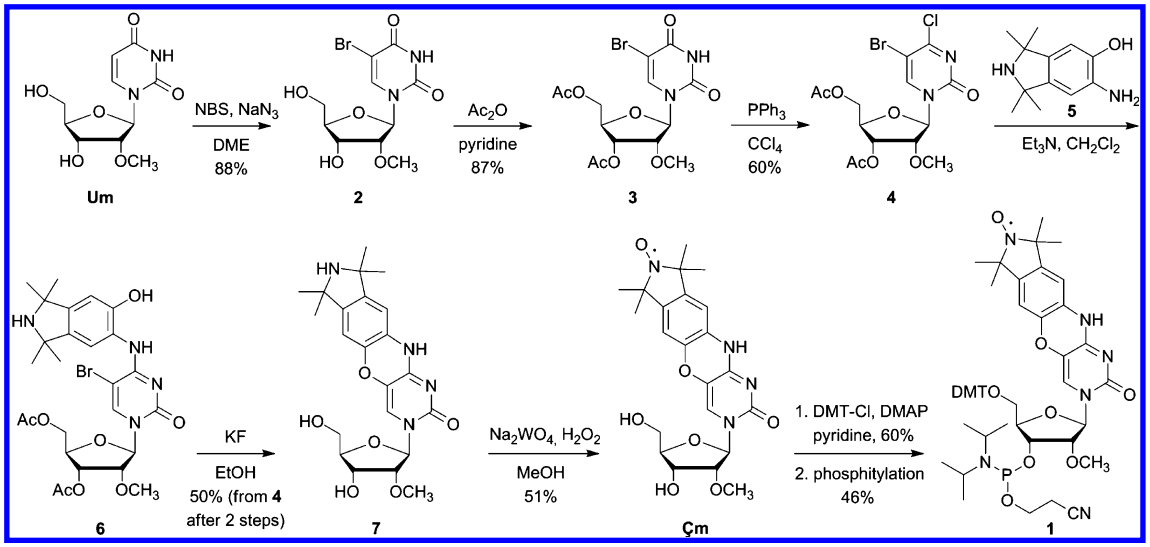

potassium fluoride in ethanol yielded the ring-closed phenoxazine derivative **7**. The substitution reaction of **4** with **5** was preferably carried out in the presence of triethylamine, which avoided the tedious removal of DBU before cyclization to **7**. Oxidation of compound **7** with hydrogen peroxide in the presence of sodium tungstate gave the paramagnetic nucleoside **Çm**. The 5′-hydroxyl group was protected as 4,4′-dimethoxytrityl ether using DMT-Cl and DMAP in pyridine. Subsequent 3′-phosphitylation in the presence of *N*,*N*-diisopropyl ammonium tetrazolide and 2-cyanoethyl *N*,*N*,*N*′,*N*′-tetraisopropyldiamidophosphite yielded the **Çm** phosphoramidite **1**, which was used for incorporation of **Çm** into RNA oligonucleotides by solid-phase synthesis.

Tetramethyl-substituted nitroxyl radicals are moderately sensitive to the conditions encountered during oxidation and detritylation in the standard solid-phase synthesis cycle.[10,20,24] Replacing the generally used iodine oxidation reagent with tBuOOH and employing dichloroacetic acid instead of trichloroacetic acid for detritylation have been shown to reduce decomposition of nitroxides during DNA synthesis.[20] We have successfully adapted the tBuOOH oxidation conditions to render the incorporation of spin-labeled phosphoramidite **1** compatible with RNA synthesis using 2′-*O*-TOM-protected RNA phosphoramidites. After completion of the synthesis, cleavage from solid support, deprotection of nucleobases and phosphates was performed with methylamine, and the 2′-*O*-TOM groups were removed by treatment with TBAF. The RNA oligonucleotides were purified by anion exchange HPLC and characterized by ESI-MS (Table S1 and Figure S1 in the Supporting Information).

The efficient incorporation of **Çm** into RNA was first demonstrated by synthesis of the 14-mer oligoribonucleotide **8Çm** (Figure 2a). Thermodynamic analysis by UV melting experiments determined the influence of **Çm** on duplex stability. The 14-mer **Çm**-labeled duplex (**8Çm**+**9**) showed a decrease in melting temperature by only 1.5−2.5 °C at various concentrations between 1 and 30 μM, compared to the unmodified (**8C**+**9**) or 2′-*O*-methylcytidine (**Cm**)-containing duplexes (**8Cm**+**9**) (Table 1 and Figure S2). On the basis of van't Hoff analysis of concentration-dependent melting curves, the difference in T_m translates into a $\Delta\Delta G^{298}$ of 4.0 kcal/mol compared to the unmodified RNA (Figure S2 and Table S2).

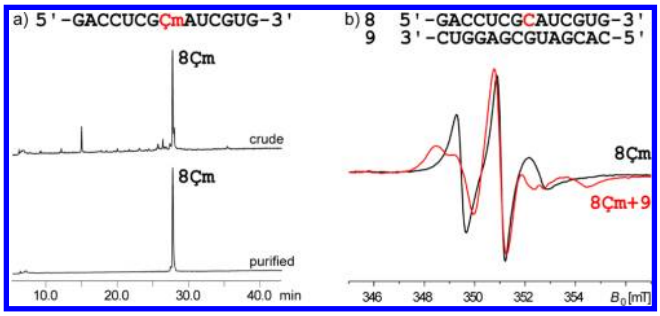

Figure 2. (a) Anion exchange HPLC of crude and purified **Çm**-labeled RNA **8**. (b) CW-EPR spectra of single-stranded **8Çm** and duplex **8Çm**+**9**.

Analysis of the duplex conformation by CD spectroscopy showed a slightly shifted and decreased maximum of the ellipticity (Figure S3). This small difference compared to the unmodified RNA is consistent with the spin label **Çm** being well tolerated in an A-form helix, indicating that the extension of the nucleobase is well accommodated in the major groove of the double helix.

The new spin label **Çm** was then incorporated into a series of mono- and bimolecular RNA structures (Figure 3), and its properties were compared to the previously reported more flexible RNA spin label $\mathbf{C}^{\mathbf{T}}$.[11] The spin labels **Çm** and $\mathbf{C}^{\mathbf{T}}$, as well as the diamagnetic **Cm**, were individually incorporated either at nucleotide C6 of the 20-mer RNA, giving the single-labeled RNAs **10a**, or simultaneously at C6 and C16, yielding the double-labeled RNAs **10b**. The complementary RNA **11** was modified at C7′ (primed numbers used for RNA **11**), resulting in the oligonucleotide **11a**. RNAs **10** and **11** are partially self-complementary and can therefore fold into hairpins (with four unpaired nucleotides at the 3′ or the 5′ terminus). The unpaired overhangs of **10** and **11** can hybridize to those of hairpins **12** and **13**, respectively, which results in the formation of bimolecular dumbbell structures (**10**+**12** and **11**+**13**). Using different combinations of RNAs **10**, **10a**, **10b**, **11**, and **11a**, four spin-labeled duplex samples were studied: two samples with a single label at position C6 or C7′, and two double-labeled duplexes with labels at nucleotides C6 and C16 and C6 and C7′, respectively.

dx.doi.org/10.1021/jo301227w | J. Org. Chem. 2012, 77, 7749−7754

Table 1. UV Melting Analysis

RNA		C	Cm		Çm		C^T[d]	
		T_m[a]	T_m[a]	ΔT_m[b]	T_m[a]	ΔT_m[c]	T_m[a]	ΔT_m[b]
8+9	D	75.1	76.0	+0.9	73.5	−1.6/−2.5	nd	nd
10a+11	D	82.2	83.9	+1.7	81.8	−0.4/−2.1	75.1	−7.1
10b+11	D	82.2	85.5	+3.3 (+1.7)	80.1	−2.1/−5.4 (−1.1/−2.7)	69.4	−12.8 (−6.4)
10a+11a	D	82.2	82.5	+0.3 (+0.2)	78.3	−3.9/−4.2 (−1.9/−2.1)	nd	nd
10+11a	D	82.2	83.1	+0.9	84.0	+1.7/+0.9	nd	nd
10a	H	88.2	88.5	+0.3	88.8	+0.6/+0.3	75.4	−12.8
10b	H	88.2	89.5	+1.3 (+0.7)	89.7	+1.5/+0.2 (+0.8/0.1)	62.7	−25.5 (−12.8)
11a	H	76.4	77.8	+1.4	73.4	−3.0/−4.4	nd	nd

[a]Melting temperature in °C (±0.5 °C). [b]ΔT_m to unmodified RNA. [c]ΔT_m to unmodified/**Cm**-modified RNA (ΔT_m per modification is given in parentheses). [d]Data from ref 11. D, duplex; H, hairpin; nd, not determined.

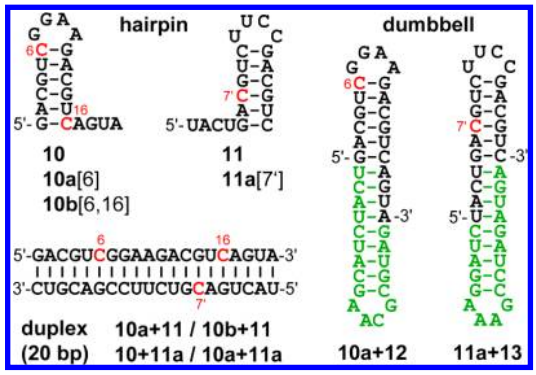

Figure 3. Sequences and secondary structures of RNAs. Individually modified cytidines are indicated in red. Modified (**Cm**-, $\mathbf{C^T}$-, and **Çm**-containing) and unmodified RNA oligonucleotides are in black and green, respectively.

The influence of the spin labels on the stability of the hairpin and duplex structures was assayed by UV melting experiments (Table 1, Figures S4 and S5). Only minor changes in T_m of less than +1 °C per spin label were observed for the hairpins **10aÇm** and **10bÇm**, indicating that **Çm** is well accommodated at the loop closing and the terminal base pair of the hairpin stem. Placing **Çm** at an internal base pair in the stem of **11a** resulted in a moderate destabilization by 3 °C. In all of the bimolecular duplex structures, the change in T_m caused by **Çm** was less than ±2 °C per modification relative to the unmodified RNA. The slightly different effects of **Çm** at different positions of the same duplex sequence most likely reflect flanking-sequence dependence, previously observed with phenoxazine derivatives in DNA.[20,25]

By comparison of the T_m values with the analogous **Cm**-modified RNAs, the effect of the extended tetracyclic nucleobase was extracted. As expected, the 2′-OMe group has a positive effect on the overall stability of the **Çm**-modified RNA, likely due to preorganization of the ribose in the north-type C3′-endo sugar conformation as usually found in RNA duplexes.[26] Thus, the destabilizing effect of the nucleobase modification is counter-balanced by the 2′-ribose modification. The comparison of the new label **Çm** with the more flexible RNA label $\mathbf{C^T}$[11] reveals considerably less destabilization by **Çm** (Table 1). This demonstrates that **Çm** is better tolerated than $\mathbf{C^T}$ in the investigated hairpin and duplex structures.

The spin-labeled RNA structures were then examined by EPR spectroscopy. The continuous wave (CW)-EPR spectra of the single-stranded RNA **8Çm** and the duplex **8Çm+9** are shown in Figure 2b. The line shape of the duplex CW-EPR spectrum is characteristic for the slow-motion regime of nitroxyl radicals in spin-labeled proteins[27] and oligonucleotides and compares well with the reported label **Ç** in an analogous DNA sequence (Figure S6).[19] This observation validates the rigidity of **Çm** and its restricted motion in an RNA duplex, due to base pairing and stacking interactions. In contrast, the line shape of the CW-EPR spectrum of the single-stranded RNA **8Çm** reflects intermediate mobility, as expected for a flexible and unstructured single strand containing a rigid spin label.[20]

The CW-EPR spectrum of the **Çm**-labeled hairpin **10aÇm** exhibited three resolved hyperfine lines (Figure 4A), with a

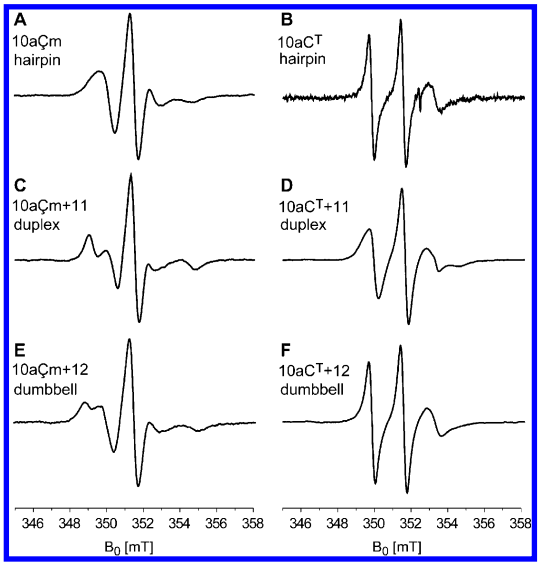

Figure 4. CW-EPR spectra of $\mathbf{C^T}$ and **Çm** spin-labeled RNAs in different secondary structure contexts.

significantly broader line shape than the $\mathbf{C^T}$-labeled hairpin RNA **10aC^T** (Figure 4B). The **Çm**- and $\mathbf{C^T}$-labeled duplexes (Figure 4C,D) show additional broadening, due to their increased size and associated slower rotational correlation times. The observed hyperfine splitting of 177 MHz for the **Çm**-labeled duplex (Figure 4C) is typical for rigid nitroxides[19,27] and characteristic for the slow-motion regime of nitroxide labels with correlation times in the range of 10 ns.[28] In contrast, such large splitting was not observed for the $\mathbf{C^T}$-labeled duplex (Figure 4D); the detected line shape reflects a correlation time on the order of 5 ns.[28] Analogous effects were observed for hairpin and duplex structures containing RNAs **10bÇm** and **11aÇm** (Figure S7A–D). A summary of the

dx.doi.org/10.1021/jo301227w | J. Org. Chem. 2012, 77, 7749–7754

characteristic hyperfine splitting values $2A_{zz}$ (separation between low- and high-field resonances) and the widths of the central lines ΔH_0 are reported in Table S3 and Figure S8. A comparison of the CW-EPR spectra of **Çm** and $\mathbf{C}^{\mathbf{T}}$-labeled hairpin and duplex RNAs at 22 and 10 °C (Figure S9) suggests that the new label **Çm** may be used to detect temperature-dependent changes in local base pair dynamics that are not reported by $\mathbf{C}^{\mathbf{T}}$.

To further examine RNA secondary structures with **Çm**, we explored the formation of bimolecular dumbbell structures, which contain the spin-labeled hairpins **10a** and **11a**. As expected, the CW-EPR line shapes of the **Çm**-labeled dumbbells **10aÇm+12** and **11aÇm+13** (Figure 4E, Figure S7E) reflect again the strongly restricted mobility of the spin label **Çm**, whereas the spectrum of the $\mathbf{C}^{\mathbf{T}}$-labeled dumbbell (Figure 4F) is insignificantly different from the hairpin spectrum. The visible spectral broadening for **Çm**-labeled dumbbells (compared to hairpins) is consistent with a decreased rotational correlation time due to the extended length of the base-paired stem upon hybridization of the complementary overhangs. We have used this effect to distinguish interacting from noninteracting RNA sequences. For example, the identical single-stranded overhangs of hairpins **10aÇm** and **13** cannot interact via standard Watson−Crick base pairs. Therefore, upon mixing **10a** and **13**, the monomolecular hairpin structures remain intact and display an unchanged CW-EPR spectrum (i.e., no dumbbell is formed, Figure S7F). In an additional set of experiments, we explored trimolecular RNA structures, in which RNA **11a** was hybridized with 2 equiv of short unlabeled RNAs (Figure S10). These trimolecular structures are essentially duplexes with gap(s). A duplex containing a four-nucleotide gap had considerably higher mobility than a duplex containing a single-nucleotide gap, demonstrating the sensitivity of the **Çm** probe for evaluating the flexibility of hinges/junctions between two helical regions.

The **Çm** label is also well suited for pulsed EPR experiments, for example, to explore RNA structures by measuring interspin distances. Additionally, the rigid spin label **Çm** provides strong orientation selection in the distance measurements. This allows for determination of orientations even at low EPR frequency (9 GHz), as already shown for **Ç**-labeled DNA duplexes,[12,22] but it also complicates the distance analysis. Pulsed electron double resonance (PELDOR) experiments with RNA samples containing two **Çm** labels provided distance results that are in agreement with estimations for typical A-form RNA helices (Figure S11). An extensive high-field pulsed EPR study of **Çm**-labeled RNA for distance and orientation measurements will be reported in due course.

In summary, we have synthesized nucleoside **Çm** containing a rigid nitroxide spin label, incorporated it into different RNA structural contexts by solid-phase synthesis, and analyzed the spin-labeled RNA by UV, CD, and EPR spectroscopy. In several aspects, **Çm** compared favorably with the more flexible label $\mathbf{C}^{\mathbf{T}}$ and other previously reported spin probes for RNA. The new label **Çm** was well tolerated in A-form helices, as judged by its small influence on the thermodynamic stability of labeled RNAs. By CW-EPR spectroscopy, **Çm** reported on the local environment of the labeling site and provided information on the global RNA structure (hairpin versus duplex or dumbbell). The rigid RNA label will be applicable not only to study intermolecular interactions but will also prove useful for sensing intramolecular refolding events or changes in the local environment of the spin probe. In addition, **Çm** will be highly valuable for orientation selection experiments that allow determination of the relative orientation of spin labels within biomolecules. This will enable the structural and dynamic characterization of larger multihelix RNAs, which are of current interest as regulators of gene expression and components of RNA maturation machineries.

EXPERIMENTAL SECTION

General. Thin layer chromatography (TLC) was carried out using glass plates precoated with silica gel (0.25 mm, F-254). Compounds were visualized by UV light and staining with *p*-anisaldehyde. Flash column chromatography was performed using ultrapure flash silica gel (230−400 mesh size, 60 Å). Dichloromethane and pyridine were freshly distilled from calcium hydride prior to use. Anhydrous triethylamine, *n*-hexane, and ethyl acetate were used without further purification. All moisture- and air-sensitive reactions were carried out in oven-dried glassware under an inert argon atmosphere. NMR spectra were recorded on a 400 MHz spectrometer. Commercial grade $CDCl_3$ was passed over basic alumina shortly before use with tritylated compounds. ^{1}H NMR chemical shifts are reported in reference to undeuterated residual solvent in $CDCl_3$ (7.26 ppm), DMSO-d_6 (2.50 ppm), and MeOH-d_4 (3.31 and 4.84 ppm). ^{13}C NMR chemical shifts are reported in reference to solvent signal ($CDCl_3$ (77.16 ppm), DMSO-d_6 (39.43 ppm), and MeOH-d_4 (49.05 ppm)). ^{31}P NMR chemical shifts are reported relative to 85% H_3PO_4 as an external standard. NMR spectra of nitroxide-containing compounds show significant broadening, sometimes to the extent that some nuclei are not observed in the spectra. For the same reason, integration of ^{1}H NMR spectra of nitroxides is not reported. Mass spectrometric analyses of all organic compounds were performed on an HR-ESI-MS (MicroTof-Q) in positive ion mode.

5-Bromo-2′-*O*-methyluridine (2). To a suspension of 2′-*O*-methyluridine (**Um**, 2.00 g, 7.74 mmol) in 1,2-dimethoxyethane (43 mL) was added a solution of NaN_3 (2.51 g, 38.7 mmol) in water (3.2 mL). [Note: NaN_3 is toxic and hazardous to the environment, and bulk quantities pose an explosion hazard.] The resulting mixture was stirred for 15 min at 22 °C and treated with *N*-bromosuccinimide (1.79 g, 10.0 mmol). The reaction mixture was stirred for 24 h at 22 °C. The solvent was removed in vacuo and the residue passed through a short silica gel column (CH_2Cl_2/MeOH; 100:0 to 95:5) to yield 5-bromo-2′-*O*-methyluridine (**2**) as a white solid (2.30 g, 88% yield): mp 223−225 °C; ^{1}H NMR (DMSO-d_6) δ 3.39 (s, 3H), 3.56−3.61 (m, 1H), 3.68−3.73 (m, 1H), 4.10−4.13 (dd, J = 5.3 Hz, 11.1 Hz, 1H), 5.12−5.14 (d, J = 6.3 Hz, 1H), 5.32−5.34 (t, J = 4.6 Hz, 9.2 Hz, 1H), 5.79 (d, J = 3.8 Hz, 1H), 8.53 (s, 1H), 11.83 (br s, 1H); ^{13}C NMR (DMSO-d_6) 57.5, 59.5, 67.7, 82.9, 84.7, 86.6, 95.7, 140.0, 149.6, 159.1; HR-ESI-MS m/z calcd for $C_{10}H_{13}BrN_2O_6$ $(M + Na)^+$ 358.9849, found 358.9841.

3′,5′-Diacetyl-5-bromo-2′-*O*-methyluridine (3). Acetic anhydride (4.18 mL, 41.1 mmol) was added to a solution of **2** (2.30 g, 6.84 mmol) in dry pyridine (5.52 mL) at 0 °C. The reaction mixture was stirred at 22 °C for 16 h, and the solvent was removed in vacuo. The residue was dissolved in CH_2Cl_2 (70 mL) and washed with water (3 × 70 mL). The organic layer was dried over anhydrous Na_2SO_4, filtered, and concentrated to give the crude product, which was purified by column chromatography (CH_2Cl_2/MeOH; 100:0 to 97:3) to yield compound **3** as a white solid (2.50 g, 87% yield): mp 162−164 °C; ^{1}H NMR ($CDCl_3$) δ 2.15 (s, 3H), 2.23 (s, 3H), 3.51 (s, 3H), 4.03−4.05 (dd, J = 2.5 Hz, 5.1 Hz, 1H), 4.38−4.43 (m, 3H), 4.94 (dd, J = 7.2, 5.3 Hz, 1H), 5.93 (d, J = 2.5 Hz, 1H), 7.97 (s, 1H), 9.29 (br s, 1H); ^{13}C NMR ($CDCl_3$) δ 20.6, 21.1, 59.1, 61.8, 69.3, 79.3, 81.9, 88.5, 97.2, 138.5, 149.3, 158.6, 170.1, 170.2; HR-ESI-MS m/z calcd for $C_{14}H_{17}BrN_2O_8$ $(M + Na)^+$ 443.0060, found 443.0068.

Compound 4. A solution of compound **3** (0.50 g, 1.19 mmol) and PPh_3 (0.78 g, 2.97 mmol), in a mixture of CH_2Cl_2 and CCl_4 (7 + 7 mL), was refluxed for 2.5 h. The solvent was removed in vacuo, and the residue was purified by silica gel flash column chromatography using a gradient elution (EtOAc/CH_2Cl_2; 5:95 to 15:85) to yield

dx.doi.org/10.1021/jo301227w | J. Org. Chem. 2012, 77, 7749−7754

compound **4** as a white solid (0.31 g, 60% yield): mp 66−68 °C; ^{1}H NMR ($CDCl_3$) δ 2.14 (s, 3H), 2.23 (s, 3H), 3.63 (s, 3H), 4.12−4.14 (d, J = 4.9 Hz, 1H), 4.42−4.55 (m, 3H), 4.75−4.78 (dd, J = 4.5 Hz, 9.5 Hz, 1H), 5.89 (s, 1H), 8.39 (s, 1H); ^{13}C NMR ($CDCl_3$) δ 20.5, 21.1, 59.2, 61.0, 68.5, 79.1, 81.5, 90.1, 97.5, 143.7, 151.4, 166.1, 170.0, 170.1; HR-ESI-MS m/z calcd for $C_{14}H_{16}BrClN_2O_7$ $(M + Na)^+$ 460.9722, found 460.9730.

Compound 6. A solution of compounds **5**[19] (87 mg, 0.42 mmol) and **4** (223 mg, 0.51 mmol) in CH_2Cl_2 (10 mL) was treated with Et_3N (55.5 mg, 0.55 mmol) at 22 °C. After 16 h, the solvent was removed in vacuo and the crude product was used directly for the next reaction without further purification.

Compound 7. KF (245 mg, 4.22 mmol) was added to a solution of compound **6** (257 mg, 0.42 mmol crude from previous step) in absolute ethanol (32 mL). After refluxing for 5 days, the solution was filtered and the solvent was removed in vacuo. The product was purified by silica gel flash column chromatography (CH_2Cl_2/MeOH; 100:0 to 65:35) to yield **7** as dark yellow solid (93 mg, 50% yield): mp (decomp.) 160−162 °C; ^{1}H NMR (MeOH-d_4) δ 1.44 (d, J = 1.2 Hz, 12H), 3.57 (s, 3H), 3.74−3.84 (m, 2H), 3.91−3.97 (m, 2H), 4.21−4.24 (dd, J = 6.8 Hz, 5.17 Hz, 1H), 5.89 (d, J = 2.6 Hz), 6.60−6.61 (d, J = 4.1 Hz, 2H), 7.86 (s, 1H); ^{13}C NMR (MeOH-d_4) δ 31.0, 31.1, 58.9, 61.1, 64.9, 64.9, 69.3, 85.5, 89.6, 109.6, 110.7, 123.7, 127.8, 129.6, 143.7, 144.1, 144.6, 155.9, 156.3; HR-ESI-MS m/z calcd for $C_{22}H_{28}N_4O_6$ $(M + H)^+$ 445.2082, found 445.2093.

Rigid Spin Label Çm. A solution of **7** (90 mg, 0.20 mmol) in MeOH (5.5 mL), containing $NaHCO_3$ (17 mg, 0.20 mmol), was treated dropwise with H_2O_2 (70% w/v, 1.11 g/mL, 0.06 mL, 1.42 mmol). After 5 min, Na_2WO_4 (10 mg, 0.03 mmol) was added and the resulting mixture was stirred for 30 h at 22 °C. The salts were filtered and discarded, the filtrate was concentrated in vacuo, and the residue was purified by flash column chromatography (CH_2Cl_2/MeOH; 100:0 to 85:15) to yield **Çm** as a yellow solid (47 mg, 51% yield): mp (decomp.) 230−232 °C; ^{1}H NMR (DMSO-d_6) δ 2.08 (br s), 3.41 (br s), 3.70 (br s), 3.85 (br s), 4.13 (br s), 5.09 (br s), 5.26 (br s), 5.88 (br s), 7.52 (br s), 8.54 (s), 10.72 (br s); ^{13}C NMR (DMSO-d_6) δ 30.5, 57.3, 59.6, 67.5, 82.8, 84.0, 86.0, 86.2, 95.4, 125.2, 139.6, 149.2, 151.2, 151.4, 158.6; HR-ESI-MS m/z calcd for $C_{22}H_{27}N_4O_7$ $(M + Na)^+$ 482.1772, found 482.1785.

5′-(4,4′-Dimethoxytrityl) Çm. Spin-labeled nucleoside **Çm** (20.0 mg, 0.04 mmol), DMTCl (22.1 mg, 0.06 mmol), and DMAP (0.6 mg, 0.004 mmol) were added to a round-bottom flask and kept under vacuum for 16 h. Anhydrous pyridine (1 mL) was added, and the resulting solution was stirred for 4 h, after which MeOH (100 μL) was added and the solvent removed in vacuo. The residue was purified by column chromatography (Et_3N/CH_2Cl_2/MeOH; 1:99:0 to 1:95:4) to yield tritylated **Çm** as a yellow solid (20 mg, 60% yield): mp (decomp.) 150−152 °C; ^{1}H NMR (DMSO-d_6) δ 3.45 (br s), 3.74 (br s), 3.96 (br s), 4.25 (br s), 5.19 (br s), 5.83 (br s), 6.93 (br s), 7.33−7.44 (br s), 10.65 (br s); ^{13}C NMR (DMSO-d_6) δ 57.6, 62.1, 68.1, 82.0, 82.7, 85.6, 86.9, 113.0, 113.1, 126.6, 127.6, 127.6, 127.7, 127.8, 129.4, 129.5, 135.1, 135.4, 144.2, 157.8; HR-ESI-MS m/z calcd $C_{43}H_{45}N_4O_9$ $(M + Na)^+$ 784.3079, found 784.3083.

Çm Phosphoramidite (1). Diisopropyl ammonium tetrazolide (24 mg, 0.14 mmol) and tritylated **Çm** (70.0 mg, 0.09 mmol) were dissolved in pyridine, the pyridine was removed in vacuo, and the residue was kept under vacuum for 16 h. CH_2Cl_2 (4 mL) was added, along with 2-cyanoethyl *N,N,N′,N′*-tetraisopropyldiamidophosphite (88 μL, 0.28 mmol), and the resulting solution was stirred for 5 h at 22 °C. CH_2Cl_2 (10 mL) was added, and the organic phase was washed with saturated aqueous $NaHCO_3$ (3 × 15 mL) and saturated aqueous NaCl (3 × 15 mL), dried over Na_2SO_4, and concentrated in vacuo. The residue was dissolved in a minimum amount of diethyl ether (7−9 mL), followed by a slow addition of hexane (40−50 mL) at 22 °C. The solvent was decanted and discarded. Finally, the compound was purified by column chromatography using neutral silica gel (EtOAc) to yield **1** as a yellow solid (40 mg, 46% yield): mp (decomp.) 130−132 °C; ^{1}H NMR ($CDCl_3$) δ 1.24−1.63 (br m), 2.82 (br s), 3.04 (br s), 4.15 (br s), 4.50 (br s), 4.64 (br s), 4.87 (br s), 5.10 (br s), 5.62 (br s), 6.42 (br s), 7.26 (br s), 7.82 (br s); ^{31}P NMR ($CDCl_3$) δ 150.59, 152.09; HR-ESI-MS m/z calcd $C_{52}H_{62}N_6O_{10}P$ $(M + Na)^+$ 984.4157, found 984.4191.

RNA Synthesis, Purification, and Characterization. RNA solid-phase syntheses were performed on a Pharmacia Gene Assembler Plus, using polystyrene custom primer support from GE Healthcare. 2′-*O*-TOM-protected ribonucleoside phosphoramidites were used for all unmodified RNA nucleotide positions. **C**^{T}-modified RNA was prepared as previously described using a convertible O^4-(4-chlorophenyl)uridine phosphoramidite.[11] **Çm**-modified RNA was synthesized using phosphoramidite **1**. Since the **Çm** phosphoramidite **1** had limited solubility in acetonitrile, it was dissolved at a concentration of 100 mM in 1,2-dichloroethane. The coupling time was set to 3 min using 250 mM benzylthiotetrazole as a coupling agent. Oxidation was performed with 1 M *tert*-butylhydroperoxide in toluene, inspired by recent reports on the stability of **Ç** under these conditions.[20] Capping and detritylation were performed under standard conditions for RNA synthesis with 2′-*O*-TOM phosphoramidites. The **Çm**-containing RNA oligonucleotides were deprotected by treatment with 8 M methylamine in ethanol/H_2O 1/1 at 37 °C for 5−6 h, followed by 2′-*O*-TOM deprotection with 1 M tetrabutylammonium fluoride (TBAF) in THF at 25 °C for 12−16 h. After desalting on a Sephadex G10 column, the quality of the crude product was checked by analytical anion exchange HPLC on a Dionex DNAPac PA200 column, 4.6 × 250 mm, flow rate 1 mL/min, 80 °C, buffer A: 25 mM Tris·HCl pH 8.0, 6 M urea; buffer B: buffer A + 0.5 M $NaClO_4$, linear gradient of B in A, with a slope of 4% per column volume. RNA oligonucleotides were purified by semipreparative anion exchange HPLC under denaturing conditions on a Dionex DNAPac PA100 column, 9 × 250 mm, flow rate 2 mL/min, 80 °C, buffers A and B as for analytical column. Detection was by UV absorbance at 280 nm. Fractions containing full-length RNA were collected and desalted on SepPak cartridges (Waters). RNA concentration was determined by UV absorbance at 260 nm, and the product identity was confirmed by ESI-MS (Table S1). RNA samples were stored as aqueous solutions at −20 °C.

Melting curves were measured in 10 mM potassium phosphate buffer, pH 7.0, 150 mM NaCl, on a Cary 100 UV spectrophotometer (Varian Inc.) equipped with a multiple cell holder and a Peltier temperature-control device. RNA sample concentration was from 2 to 40 μM. Temperature-dependent changes in UV absorbance were measured at 250, 260, 270, and 280 nm, with a heating/cooling rate of 0.7 °C/min. Two full heating and cooling cycles (4 ramps) were collected, and all melting transitions were fully reversible and reproducible. Thermodynamic parameters for the duplices **8**+**9** were obtained from concentration-dependent melting curves by analysis of $\ln(c_T)$ versus $1/T_m$.

CD spectra were recorded on a Chirascan CD spectrophotometer (Applied Photophysics) at an RNA duplex concentration of 10 or 40 μM in 10 mM potassium phosphate buffer, pH 7.0, 150 mM NaCl, at 25 °C, with 0.5 nm step size and 2 s/data point. Data were collected in three repetitions and averaged. CD spectra are depicted in Supporting Information Figures S1 and S3.

EPR Experiments. Aliquots of RNA samples were lyophilized and dissolved in buffer. The buffer composition was 10 mM potassium phosphate buffer, pH 7.0 containing 150 mM NaCl. The final concentration of the spin-labeled RNA was 10−25 μM. For bimolecular samples with only one spin-labeled strand, the unmodified complementary strand was used in 1.5-fold excess; for the trimolecular constructs, the short unmodified strand (**14** or **15**) was in 10-fold excess. For the duplex sample containing two single-labeled strands, equimolar amounts of **10a**+**11a** were used. All samples were heated to 90 °C for 3 min and slowly cooled to 22 °C. The EPR samples (15 μL) were placed in quartz capillaries sealed at one end. CW-EPR spectra were recorded at 23 °C at X-band (9 GHz) over 160 G on a Bruker Elexsys 500 spectrometer fitted with a high-sensitivity resonator using 20 mW incident microwave power and 1 G field modulation amplitude at 100 kHz modulation frequency. From the CW-EPR spectra, the peak-to-peak line width of the central line (ΔH_0, in mT) and the separation between the resonances of the low- and high-field lines ($2A_{zz}$, in mT) were extracted (Supporting Table S3)

dx.doi.org/10.1021/jo301227w | J. Org. Chem. 2012, 77, 7749−7754

and plotted as a function of the number of base pairs (Supporting Figure S6).

■ ASSOCIATED CONTENT

Ⓢ Supporting Information

List of abbreviations, Supporting Tables S1−S3, Supporting Figures S1−S11, copies of ^{1}H and ^{13}C NMR spectra for compounds **2**−**7**, **Çm**, and DMT **Çm**, ^{1}H and ^{31}P NMR spectra for phosphoramidite **1**. This material is available free of charge via the Internet at http://pubs.acs.org.

■ AUTHOR INFORMATION

Corresponding Author

*E-mail: claudia.hoebartner@mpibpc.mpg.de, snorrisi@hi.is.

Notes

The authors declare no competing financial interest.

■ ACKNOWLEDGMENTS

Prof. Marina Bennati (MPIbpc, Research Group Electron Paramagnetic Resonance) is gratefully acknowledged for stimulating discussion and access to EPR instruments. We thank Uwe Pleßmann and Prof. Henning Urlaub (MPIbpc, Facility for mass spectrometry) for recording ESI-MS spectra of RNA oligonucleotides, and Brigitta Angerstein for help with EPR sample preparation. This work was supported by the Max Planck Society and the Icelandic Research Fund (090026023).

■ REFERENCES

(1) Sowa, G. Z.; Qin, P. Z. *Prog. Nucleic Acid Res. Mol. Biol.* **2008**, *82*, 147.
(2) Longhi, S.; Belle, V.; Fournel, A.; Guigliarelli, B.; Carriere, F. *J. Pept. Sci.* **2011**, *17*, 315.
(3) Krstic, I.; Endeward, B.; Margraf, D.; Marko, A.; Prisner, T. F. *Top. Curr. Chem.* **2012**, *321*, 159.
(4) Shelke, S. A.; Sigurdsson, S. T. *Eur. J. Org. Chem.* **2012**, 2291.
(5) Edwards, T. E.; Okonogi, T. M.; Robinson, B. H.; Sigurdsson, S. T. *J. Am. Chem. Soc.* **2001**, *123*, 1527.
(6) Kim, N.-K.; Murali, A.; DeRose, V. J. *Chem. Biol.* **2004**, *11*, 939.
(7) Qin, P. Z.; Butcher, S. E.; Feigon, J.; Hubbell, W. L. *Biochemistry* **2001**, *40*, 6929.
(8) Qin, P. Z.; Haworth, I. S.; Cai, Q.; Kusnetzow, A. K.; Grant, G. P. G.; Price, E. A.; Sowa, G. Z.; Popova, A.; Herreros, B.; He, H. *Nat. Protoc.* **2007**, *2*, 2354.
(9) Schiemann, O.; Piton, N.; Mu, Y.; Stock, G.; Engels, J. W.; Prisner, T. F. *J. Am. Chem. Soc.* **2004**, *126*, 5722.
(10) Piton, N.; Mu, Y.; Stock, G.; Prisner, T. F.; Schiemann, O.; Engels, J. W. *Nucleic Acids Res.* **2007**, *35*, 3128.
(11) Sicoli, G.; Wachowius, F.; Bennati, M.; Höbartner, C. *Angew. Chem., Int. Ed.* **2010**, *49*, 6443.
(12) Schiemann, O.; Cekan, P.; Margraf, D.; Prisner, T. F.; Sigurdsson, S. T. *Angew. Chem., Int. Ed.* **2009**, *48*, 3292.
(13) Krstic, I.; Frolow, O.; Sezer, D.; Endeward, B.; Weigand, J. E.; Suess, B.; Engels, J. W.; Prisner, T. F. *J. Am. Chem. Soc.* **2010**, *132*, 1454.
(14) Wunnicke, D.; Strohbach, D.; Weigand, J. E.; Appel, B.; Feresin, E.; Suess, B.; Müller, S.; Steinhoff, H.-J. *RNA* **2011**, *17*, 182.
(15) Zhang, X.; Tung, C.-S.; Sowa, G. Z.; Hatmal, M. M.; Haworth, I. S.; Qin, P. Z. *J. Am. Chem. Soc.* **2012**, *134*, 2644.
(16) Tkach, I.; Sicoli, G.; Höbartner, C.; Bennati, M. *J. Magn. Reson.* **2011**, *209*, 341.
(17) Nguyen, P.; Qin, P. Z. *Wiley Interdiscip. Rev. RNA* **2012**, *3*, 62.
(18) Miller, T. R.; Alley, S. C.; Reese, A. W.; Solomon, M. S.; McCallister, W. V.; Mailer, C.; Robinson, B. H.; Hopkins, P. B. *J. Am. Chem. Soc.* **1995**, *117*, 9377.
(19) Barhate, N.; Cekan, P.; Massey, A. P.; Sigurdsson, S. T. *Angew. Chem., Int. Ed.* **2007**, *46*, 2655.
(20) Cekan, P.; Smith, A. L.; Barhate, N.; Robinson, B. H.; Sigurdsson, S. T. *Nucleic Acids Res.* **2008**, *36*, 5946.
(21) Cekan, P.; Jonsson, E. O.; Sigurdsson, S. T. *Nucleic Acids Res.* **2009**, *37*, 3990.
(22) Marko, A.; Denysenkov, V.; Margraf, D.; Cekan, P.; Schiemann, O.; Sigurdsson, S. T.; Prisner, T. F. *J. Am. Chem. Soc.* **2011**, *133*, 13375.
(23) Denapoli, L.; Messere, A.; Montesarchio, D.; Piccialli, G.; Santacroce, C. *Bioorg. Med. Chem. Lett.* **1992**, *2*, 315.
(24) Gannett, P. M.; Darian, E.; Powell, J.; Johnson, E. M., II; Mundoma, C.; Greenbaum, N. L.; Ramsey, C. M.; Dalal, N. S.; Budil, D. E. *Nucleic Acids Res.* **2002**, *30*, 5328.
(25) Sandin, P.; Börjesson, K.; Li, H.; Mårtensson, J.; Brown, T.; Wilhelmsson, L. M.; Albinsson, B. *Nucleic Acids Res.* **2008**, *36*, 157.
(26) Egli, M.; Pallan, P. S. *Annu. Rev. Biophys. Biomol. Struct.* **2007**, *36*, 281.
(27) Hubbell, W. L.; Cafiso, D. S.; Altenbach, C. *Nat. Struct. Biol.* **2000**, *7*, 735.
(28) Stoll, S.; Schweiger, A. *J. Magn. Reson.* **2006**, *178*, 42.